Proceedings of the 9th U.S. National and 10th Canadian Conference on Earthquake Engineering
Compte Rendu de la 9ième Conférence Nationale Américaine et
10ième Conférence Canadienne de Génie Parasismique
July 25-29, 2010, Toronto, Ontario, Canada • Paper No 1122

GEOMETRIC ATTENUATION FUNCTIONS FOR RESPONSE SPECTRA ACCOUNTING FOR SEISMOLOGICAL PARAMETERS

J. X. Zhao [1]

ABSTRACT

Attenuation models derived from recorded ground motions are still important elements of probabilistic seismic hazard studies. Many attenuation models have been published for different parts of the world and for different types of earthquakes. Most models have a simple function of source distance – constant or magnitude-dependent geometric spreading, and seldom consider well-known seismological effects such as Moho reflection for shallow crustal earthquakes, multiple travel paths and constructive interference for subduction earthquakes. In the present study, a large set of strong-motion records obtained from dense recording networks in Japan is used to derive geometric attenuation functional form. The present study proposes a set of geometric attenuation function forms to account for these well-known seismological parameters and plausible explanations of the physical process. The proposed model shows a large increase in the maximum likelihood from the random effects methodology, the elimination of bias in the distribution of residuals with respect to source distance, and much improved fitting for well-recorded earthquakes.

Introduction

Empirical attenuation models are still vital for probabilistic seismic hazards studies and many models have been developed for crustal earthquakes (Abrahamson and Silva, 2008; Boore and Atkinson, 2008; Chiou and Youngs, 2008; McVerry et al., 2006; Zhao et al., 2006a) and for subduction events (Atkinson and Boore, 2003; McVerry et al., 2006; Youngs et al., 1997; Zhao et al., 2006a). Many models have simple functional forms, such as the Zhao et al. (2006a) model, and most other models derived before the NGA project.

There are some well-known seismological effects that are seldom considered in empirical attenuation models, such as Moho reflection (Somerville et al., 1994) and multiple seismic-wave travel paths that may lead to constructive interference at recording stations in a certain range of distance. One reason for not accounting for these effects is that a large enough number of strong-motion records from densely distributed recording networks have not been available until recently. The dataset compiled by Zhao et al. (2006a) now allows a detailed study to identify

[1] Senior Engineering Seismologist, GNS Science, Lower Hutt, New Zealand

these effects and incorporate them in a set of relatively simple empirical attenuation functions. In the present study, firstly a simple model is derived and extensive residual analyses are carried out. Based on the residual analyses, a number of parameters that can possibly correct the biased distribution of residuals (with respect to source distance) are introduced, and then detailed residual analyses are carried out again. Guided by the observed data, parameters that can be linked to plausible physical and seismological mechanisms, such as Moho reflection for crustal earthquakes and multiple wave propagation paths in subduction zones, are retained. Using this approach, a preliminary model is constructed and comparisons are made with the recorded data.

Simple models for residual analysis

The following simple attenuation models are used for the purpose of residual analyses only, i.e., the simple model has all the parameters to model the first order (most important) effect, such as magnitude scaling, simple geometric spreading, anelastic attenuation, depth effect and the effect of earthquake source categories.

For crustal earthquakes (within a depth of 25km),

$$\log_e(y_{i,j}) = aM_{wi} + f_{Cr}(M_{wi}) - b_{Cr}x_{i,j} - \log_e(r_{i,j}) + e_{Cr}(h-h_c)\delta_h + F_R\delta_R + C_k + \xi_{i,j} + \eta_i \quad (1a)$$

$$f_{Cr}(M_w) = a_{Cr}(M_w - M_C)^2 \quad (1b)$$

for subduction interface earthquakes,

$$\log_e(y_{i,j}) = aM_{wi} + f_{Int}(M_{wi}) - b_{Int}x_{i,j} - \log_e(r_{i,j}) + e_{Int}(h-h_c)\delta_h + C_k + S_{Int} + \xi_{i,j} + \eta_i \quad (1c)$$

where

$$f_{Int}(M_w) = a_{Int}(M_w - M_I)^2 \quad (1d)$$

and for subduction slab earthquakes,

$$\log_e(y_{i,j}) = aM_{wi} + f_{Slb}(M_{wi}) - b_{Slb}x_{i,j} - \log_e(r_{i,j}) + e_{Slb}(h-h_c)\delta_h + C_k + S_{Slb} + \xi_{i,j} + \eta_i \quad (1e)$$

$$f_{Slb}(M_w) = a_{Slb}(M_w - M_{S1})(M_w - M_{S2})(M_w - M_{S3}) \quad (1f)$$

$$r_{i,j} = x_{i,j} + c\exp(dM_{wi}) \quad (1g)$$

$$\delta_h = \begin{cases} = 1 & h > h_c \\ = 0 & h \le h_c \end{cases} \quad (1h)$$

$$\delta_R = \begin{cases} = 1 & \text{for crustal events with reverse faulting mechanism} \\ = 0 & \text{for all other crustal events} \end{cases} \quad (1i)$$

In Equation (1), y is the acceleration spectrum at a given spectral period, M_w is the moment magnitude, x is the source distance, and b denotes the anelastic attenuation term. F_R is the term for crustal earthquakes with a reverse faulting mechanism, and C_k is the site term for site class k. S denotes the term for earthquake category, h denotes the focal depth and h_c is a depth parameter. M_C, M_I, M_{S1}, M_{S2}, and M_{S3} are magnitude constants for quadratic or cubic magnitude scaling terms (Zhao et al., 2006a). Random variables ξ and η denote the intra- and inter-event errors, respectively. The subscript *Cr* denotes shallow crustal events, the subscript *Int* denotes subduction interface events and the subscript *Slb* denotes subduction slab events. The

subscript i denotes the i^{th} event, and j denotes the j^{th} record in the i^{th} earthquake. Note that all three types of earthquakes have common near-source terms (parameters c and d), common linear magnitude term, common geometric attenuation term and common site terms. When the coefficient for magnitude squared term or magnitude cubic term is not zero, each earthquake type has a separate linear magnitude term.

Site classes are determined by Zhao et al. (2006b) and the definition of site classes is presented in Table 1.

Table 1 Site class definitions used in the present study and the approximately corresponding NEHRP site classes (BSSC 2000)

Site class	Description	Natural period	V_{30} calculated from site period	NEHRP site classes
SC I	Rock	$T < 0.2$s	$V_{30} > 600$	A+B+C
SC II	Hard soil	$0.2 = T < 0.4$s	$300 < V_{30} = 600$	C
SC III	Medium soil	$0.4 = T < 0.6$s	$200 < V_{30} = 300$	D
SC IV	Soft soil	$T \geq 0.6$s	$V_{30} \leq 200$	E+F

Because of the limited length of this manuscript, attenuation characteristics of subduction interface ground motions are not reported here.

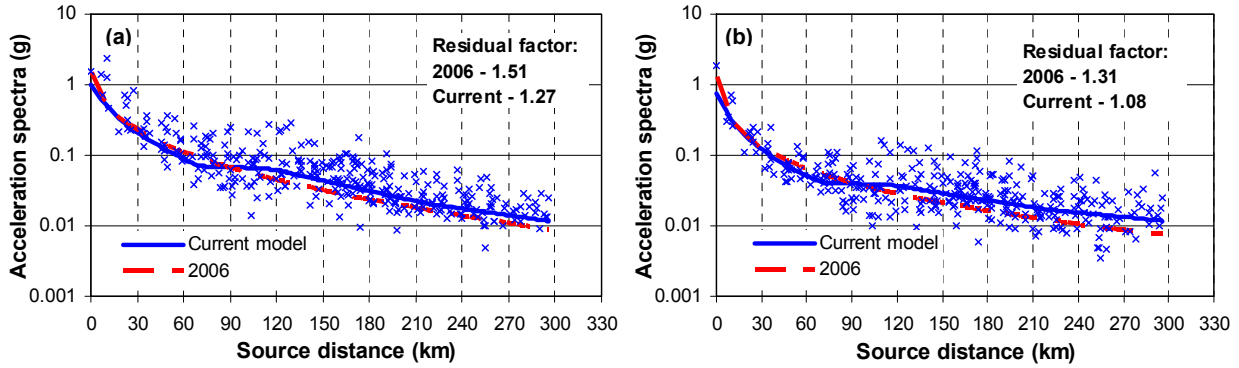

Figure 1 Attenuation of acceleration spectra with source distance for the records from the 2000 Tottori earthquake for (a) 0.4s and (b) 0.7s spectral period. The thick lines are the model predictions of the Zhao et al. (2006a) and modified model reported here (see later sections). The acceleration spectra have been normalized to have a site class SC II condition. The average residual factor is the exponential of the average total residuals.

Geometric attenuation functions for crustal earthquakes

Figure 1 shows the normalized spectra against the source distance for records from the western Tottori prefecture earthquake in 2000, a shallow crustal event with a moment magnitude of 6.65 and a depth of 10km. The response spectra are normalized to the SC II site class using the site terms derived from the present study, i.e., each spectrum from site class k is multiplied by $\exp(C_2\text{-}C_k)$. At 0.4s and 0.7s spectral periods, the variation of the normalized spectra with source distance shows clearly that, in a distance range of 70-120km, the response spectra do not

attenuate significantly with increasing distance – a possible effect of Moho reflection that is observed in Fourier spectral attenuation by Atkinson and Mereu, (1992) and many others. At distances over 200km, the attenuation rate appears to be less than that for the shorter distances.

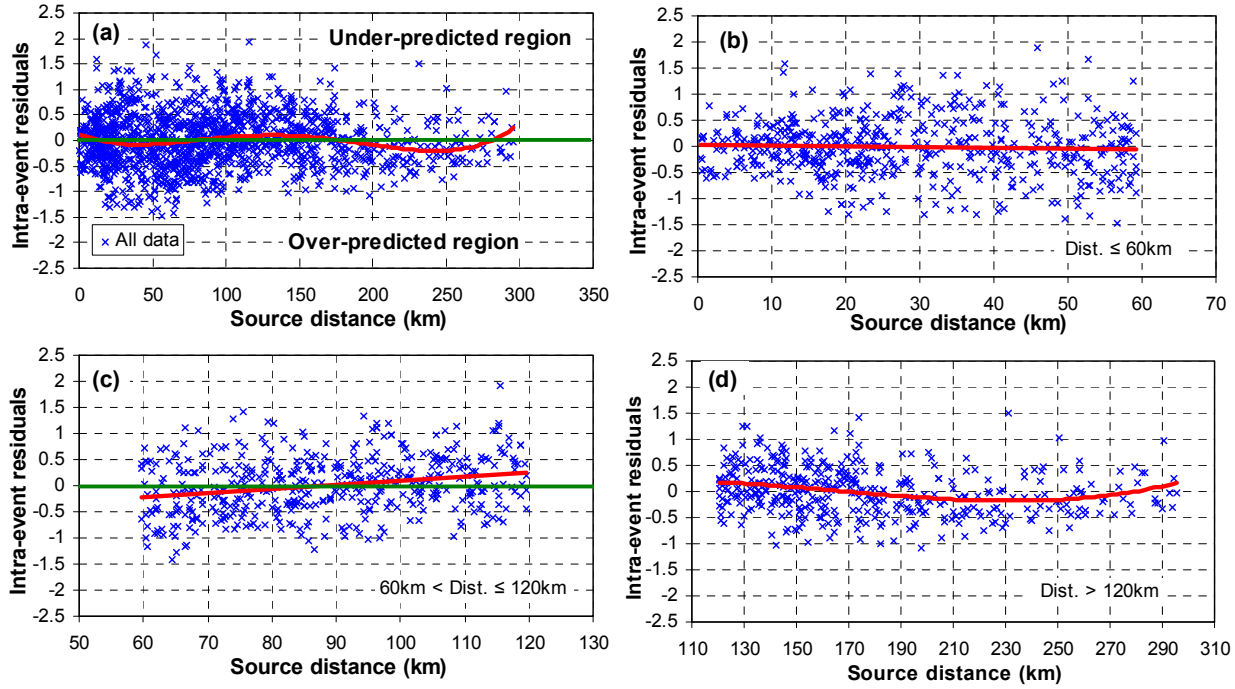

Figure 2 PGA intra-event residuals for crustal earthquake records for all data and three distance ranges. Positive residuals means under-prediction and negative residuals means over-prediction

Figure 2 shows the distribution of PGA residuals with respect to source distance for all shallow crustal events used in the Zhao et al. (2006a) model. The solid line in the residual plots is the fitted fourth order polynomial of source distance to identify the possible biased distribution of residuals with distances. Linear trend lines are used for distance range of 0-60km and 60-120km while a third order polynomial of source distance is used for data over 120km. For a 'perfect' model, the solid line fitted to the residuals should equal zero at all distance ranges. The residuals in the 60-120km range (Figure 2c) are clearly biased, with the data in a distance range of 60-80km being over-predicted on average and the data in 90-120km being under-predicted. The bias is consistent with the effect of Moho reflection. In many seismological studies on anelastic attenuation rates, the effect of Moho reflection is accounted for by using -1.0 geometric attenuation rate within a hypocentral distance of 70km (Atkinson and Mereu, 1992), zero geometric spreading in a source distance of 70-120km and -0.5 geometric attenuation rate for distances over 120km. At source distances over 120km (Figure 2d), the residuals appear to be biased, with the data at source distances over 250km being under-predicted. The under-prediction at distances over 250km may be the effect of a secondary reflection, though there is no previous study on this effect. Another possible explanation for the "apparent" under-prediction is the effect of un-triggered instruments, i.e., at a specific station, the ground motion with low amplitude within a usual variability range is not recorded, if the minimum ground motion level selected in the data is too small. For engineering applications, the ground motion from such a large distance is not very important and these data are used mainly for deriving reliable estimates of site terms, overall attenuation rates and the terms for earthquake source

types. If these distant data are used without rigorous correction for the under-prediction, the model prediction in the useful distance ranges for engineering applications may be adversely affected. Figure 2 confirms that the effect of Moho reflection appears to be present in the records not only from one event but also from other crustal earthquakes.

The following additional geometric attenuation model for shallow crustal earthquakes is proposed (-1 geometric attenuation rate is already used in Equation 1),

$$g_{Cr}(r) = \frac{h_m - h}{h_m - h_{crc}} \begin{cases} a_1 \ln(r) & for\ x \le x_1 \\ a_1 \ln(r_1) + a_2[\ln(r) - \ln(r_1)] & for\ x_1 \le x < x_2 \\ a_1 \ln(r_1) + a_2[\ln(r_2) - \ln(r_1)] + a_3[\ln(r) - \ln(r_2)] & for\ x_2 \le x < x_3 \\ a_1 \ln(r_1) + a_2[\ln(r_2) - \ln(r_1)] + a_3[\ln(r_3) - \ln(r_2)] + a_4[\ln(r) - \ln(r_3)] & for\ x \ge x_3 \end{cases} \quad (2a)$$

$$r_m = x_m + c \exp(dM_w) \qquad m = 1, 2 \text{ and } 3 \quad (2b)$$

where h is the focal depth, h_m and h_{crc} are depth terms and x_1, x_2, x_3 are distance constants. The depth scaling for the geometric attenuation term leads to $g_{Cr}(r)=0$ when $h=h_m$ and the depth scaling term equals 1.0 when $h=h_{crc}$. Note that h_{crc} is smaller than h_m and the depth scaling term is always positive because h is always less than h_m. The purpose of the depth-dependent function term is to produce a larger effect of Moho reflection for shallow earthquakes than for deep crustal earthquakes (within a depth of 25km). The effect of Moho reflection is intuitively negligible when the depth of the earthquake is close to the depth of the Moho discontinuity. According to Somerville et al., (1994), the distance where seismic waves from critical Moho reflection reach at the ground surface would decrease with increasing earthquake depth. When the reflected seismic waves reach the ground surface at a relatively close distance, the amplitude of the reflected waves may be relatively small compared with the direct arrivals, leading to a relatively small effect of Moho reflection. Equation (2) can mimic this effect but further studies are necessary to verify the depth scaling term.

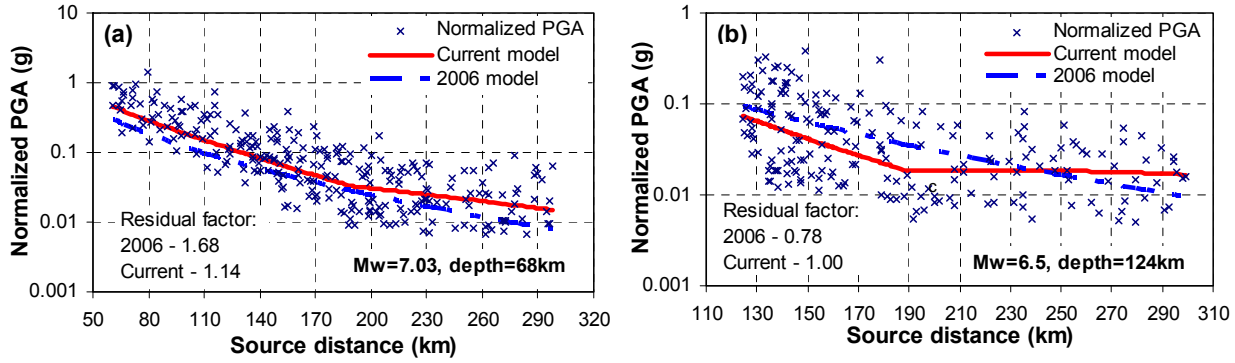

Figure 3 PGA Attenuation of spectral accelerations for two deep subduction slab earthquakes. The normalized PGA does not attenuate with increasing source distances over 200km. The thick lines are the model predictions of the Zhao et al. (2006a) and modified model reported (see later sections). The acceleration spectra have been normalized to have a site class SC II condition.

Attenuation characteristics for the subduction slab earthquakes

Figure 3 shows the normalized PGA against the source distance for two subduction slab

earthquakes with different magnitudes and focal depths. Figure 3(a) shows the normalized PGA from a subduction slab event with M_w=7.03, and a focal depth of 68km (26 May 2003). 264 records from this event are used in the present study, and this earthquake generated a few records with PGAs over 0.6g at a source distance over 50km. The normalized PGA attenuates very slowly with increasing source distance beyond about 200km. Figure 3(b) shows the normalized PGA for a very deep subduction slab event with M_w= 6.5 and a focal depth of 124km (2 December 2001). This is the only deep subduction slab event (over 80km) that was well recorded, with 208 useful records. Again, the PGA on average attenuates very slowly with increasing distance beyond 180km, and the scatter of this event is much larger than for the other subduction slab events. This earthquake generated one record with a PGA of 0.36g at a source distance of 149km and 9 records with a PGA over 0.2g in a source distance range of 130-179km. Figure 3 clearly shows that records from deep subduction earthquakes tend to either attenuate very slowly or not attenuate at all with increasing distance beyond some large threshold, and the threshold distance tends to decrease with increasing focal depth. Figure 4 shows the PGA residuals for subduction slab events with a focal depth larger than 50km and over 100km. The simple model in Equation (1) under-predicts the spectra by a very large amount at large distance, on average by a factor of 1.9 at 300km for all deep subduction events. Figure 4 also confirms that the change of attenuation rates at different distance ranges occurs in all deep slab events.

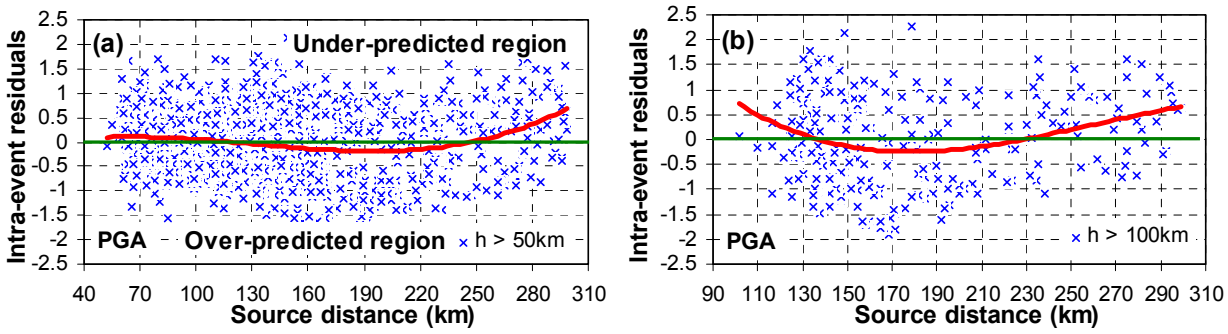

Figure 4 Distribution of residuals for deep subduction earthquakes, (a) over 50km depth and (b) over 100 km depth. Positive residuals means under-prediction and negative residuals means over-prediction. Clearly, the records at large distance are severely under-predicted

Figure 5a suggests a possible reason for the under-prediction of the ground motion resulting from the deep slab earthquakes by the simple model in Equation (1). At a station on the ground surface, the direct arrivals of seismic waves (through the shortest travel path) from a deep slab earthquake are likely to propagate through the mantle with a relatively low Q value and a low shear-wave velocity, before passing through crust that has a relatively high Q value. However, the seismic waves propagating within the slab will eventually come out of the slab (because of the bending of the slab and possible reduction in shear-wave velocity with decreasing depth) and turn left-upward. Because the shear-wave velocity of the slab is much higher than that of the mantle and that of the crust, the seismic waves propagating through the slab and the mantle will catch up with the direct arrivals at a particular source distance range, leading to possible constructive interference at some of the ground recording stations. For a deep slab event, the length of the high-Q and high-shear-wave velocity path will be much greater than for a shallow slab event, and the long high-Q path leads to the severe under-prediction of

the response spectra from a deep subduction earthquake by the simple models in Equation (1).

It is also observed that intensity isoseismals for a subduction slab event appear to attenuate much more slowly along the strike of the subduction trench than in the direction perpendicular to the strike of the slab. One possible reason is that slab events tend to have a normal or strike-slip focal mechanism and the rupture often propagates along the strike of the subduction trench. Figure 5b suggests another possible wave propagation path where seismic waves travel through a long distance within the slab in the strike direction. The constructive interference between the direct arrivals and the seismic waves that travel a long distance within the high-Q slab could lead to low apparent attenuation rates in the strike direction of the subduction plate.

The effect of Q values on the amplitude of seismic waves usually decreases with increasing period, and long period seismic waves will be attenuated mainly by geometric spreading. The changes in attenuation rates as shown in Figures 3 and 5 become negligible at long periods.

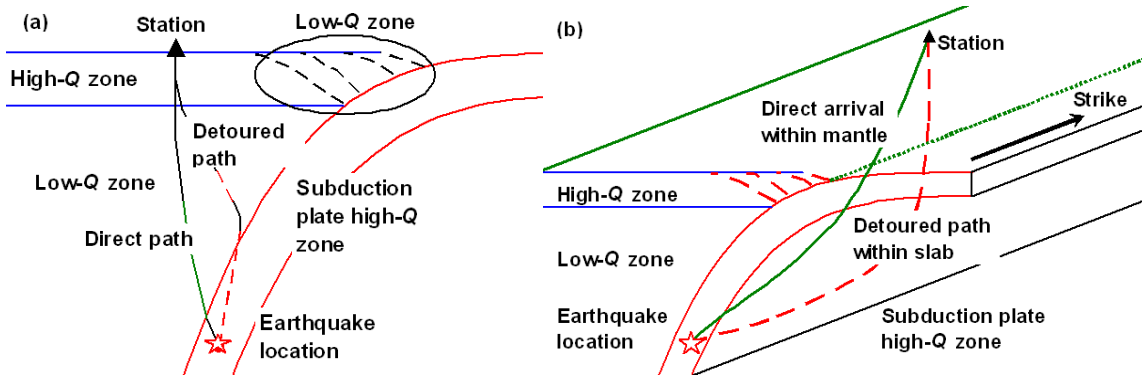

Figure 5 Possible wave propagation paths for direct arrivals and the seismic waves that travel through a long distance within the high-Q slab (detoured path), (a) upwards and (b) along the strike of the fault.

The approach by Atkinson and Mereu, (1992) for modeling the effect of Moho reflection is adopted in the present study – using separate geometric attenuation rates for different distance ranges. Both mechanisms have a common key factor that controls the apparent change of attenuation rate – a relatively large travel distance for the seismic waves in the low-Q slab (along the detoured travel path) and this key factor can be represented by a simple function of earthquake depth and source distance. The following geometric attenuation functions are proposed for subduction slab events;

$$g_{Slb1}(r) = \frac{h - h_1}{h_{Slbc} - h_1}\delta(h - h_1)$$

$$\begin{cases} a_5 \ln(r) \ for \ x \le x_4 \\ a_5 \ln(r_4) + a_6[\ln(r) - \ln(r_4)] \ for \ x_4 \le x < x_5 \\ a_5 \ln(r_4) + a_6[\ln(r_5) - \ln(r_4)] + a_7[\ln(r) - \ln(r_5)] \ for \ x \ge x_5 \end{cases} \quad (3a)$$

$$\delta(h-h_1)=\begin{cases}1 & h\geq h_1\\ 0 & h<h_1\end{cases} \qquad (3b)$$

where h_1 is a depth term, h_{Slbc} is a depth constant so that the depth scaling term equals 1.0 when $h=h_{Slbc}$, and x_4 and x_5 are distance constants. The depth term here is to represent a depth below which the seismic waves would propagate for a relatively large distance in the high-Q slab, while the seismic waves from a shallow subduction slab event may travel for a relatively small distance in the slab, for both mechanisms suggested in Figure 5. At a relatively small distance, for example, within 120km, the wave-propagation mechanism presented in Figure 5a would dominate the observed apparent change of geometric attenuation rate. The depth terms in Equations 3 are designed to model this aspect. At a distance larger than about 220km (mainly for the physical mechanism suggested in Figure 5b), the distance for the seismic waves to travel in the high-Q slab may be again relatively small compared with the total distance, and, therefore, the effect of the high-Q zone may become relatively small. The distances x_4 and x_5 are designed to model the wave-propagation mechanism suggested in Figure 5.

The residuals for long period spectra at 2.5s and 3s for shallow and deep slab events are also biased, with the shallow slab records being under-predicted at large distance and the deep slab records being over-predicted. At 3s spectral period, the simple models in Equation (1) over-predict the recorded spectra by a factor as large as 1.5 on average at a source distance of 300km. No plausible theoretical explanation can be offered for this observed change of attenuation rate at large source distance for shallow and deep slab earthquake records. The following attenuation functions are proposed for slab earthquake records (for all periods, but the values for short periods are negligible),

$$g_{Slb2}(r)=\frac{h-h_2}{h_{Slbd}-h_2}\begin{cases}a_8\ln(r) & for\ x<x_6\\ a_8\ln(r_6)+a_9[\ln(r)-\ln(r_6)] & for\ x\geq x_6\end{cases} \qquad (4)$$

where h_2 is a depth term, h_{Slbd} is a depth constant such that the depth scaling term equals 1.0 when $h= h_{Slbd}$, and x_6 is a distance constant. Note that the geometric attenuation rate changes from negative to positive when the depth of an earthquake increases from $h < h_2$ to $h > h_2$. The distance term r_m is defined by

$$r_m = x_m + c\exp(dM_w) \qquad m=4,5\text{ and }6 \qquad (5)$$

New functional forms for attenuation models and improved model prediction

For shallow crustal earthquakes, the new attenuation functions can be written as

$$\log_e(y_{i,j}) = aM_{wi} + f_{Cr}(M_{wi}) - b_{Cr}x_{i,j} - \log_e(r_{i,j}) - g_{Cr}(r_{i,j}) + e_{Cr}(h-h_c)\delta_h + F_R\delta_R + C_k + \xi_{i,j} + \eta_i \qquad (6a)$$

For subduction slab earthquakes,

$$\log_e(y_{i,j}) = aM_{wi} + f_{Slb}(M_{wi}) - b_{Slb}x_{i,j} - \log_e(r_{i,j}) + g_{Slb1}(r_{i,j}) + g_{Slb2}(r_{i,j}) + e_{Slb}(h-h_c)\delta_h + C_k + S_{Slb} + \xi_{i,j} + \eta_i \qquad (6b)$$

The distance and depth terms used in Equations 2-5 are presented in Table 2. Note that the models for crustal and subduction earthquakes are coupled together by common site terms and any bias associated with one particular type of earthquake will, to some extent, affect the model prediction for all other types of earthquake. The improved model prediction for any particular type of earthquake presented in this study will be a result of the overall modeling improvement.

The residual factor, the exponential of average total residuals (the sum of the inter- and intra-event residuals), is used as an indicator for the goodness of fit between the model and a particular group of recorded ground-motion records. The residual factor is the geometric mean of the ratio of the recorded spectra over the predicted spectra for this particular group of records at a given spectral period. If the residual factor is larger than 1.0, the recorded spectra on average are under-predicted, and, if the residual factor is less than 1.0, the recorded spectra on average are over-predicted.

Table 2 Depth and distance parameters

Depth (km)		Distance (km)	
h_m	30	x_1	70
h_c	10	x_2	120
h_1	30	x_3	220
h_2	70	x_4	120
h_{Crc}	12	x_5	190
h_{Slbc}	70	x_6	220
h_{Slbd}	80		

Figure 1 compares the predicted spectra for the western Tottori prefecture earthquake in 2000, Japan (October 2000). The predictions of the new model for spectra at 0.4s for this event are much improved, with the residual factor reduced from 1.51 in the Zhao et al. (2006a) model down to 1.27. Figure 1(b) shows that the residual factor is reduced from 1.31 to 1.08 at 0.7s. Figure 3 compares the model predictions for PGA of two well-recorded subduction slab earthquakes. The residual factor for the M_w=7.03 event in Figure 3(a) is reduced from 1.68 in the Zhao et al. (2006a) model to 1.14, a huge improvement in the model prediction. The new model has an excellent fit to the deep earthquake in Figure 3(b) with a residual factor of 1.0, compared with the residual factor of 0.78 from the Zhao et al. (2006a) model.

Summary

Through extensive residual analyses, a new set of geometric attenuation functions that accommodate well-known seismological parameters have been proposed for shallow crustal and deep subduction slab earthquakes in Japan. The possible effects of Moho reflection for crustal earthquakes and multiple seismic propagation paths for deep subduction slab earthquakes are incorporated in the proposed geometric attenuation functions. The predictions of well-recorded crustal and deep subduction earthquakes are improved significantly over those of the Zhao et al. (2006a) model.

Acknowledgement

This research was supported in part by a biennial research grant (2008) from the New Zealand Earthquake Commission, and by the Foundation for Research, Science and Technology, under programme CO5X0402. The author would like to thank Jane Forsyth and Dr. David Rhoades for reviewing the manuscript, and Professor Kojiro Irikura for his invaluable discussions and generous support. Dr. N. Abrahamson kindly offered his computer code for the random effects model that was used in the present study.

References

Abrahamson, N. A. and Silva, W. J., 2008 Summary of the Abrahamson & Silva NGA Ground-Motion Relations, *Earthquake Spectra*, Vol 24(1), 67-97

Atkinson, G.M. and Mereu, R. F., 1992, The shape of ground motion attenuation curves in southeastern Canada, *Bulletin of the Seismological Society of America*, 82, 2014-2031

Atkinson, G.M. and Boore, D.M., (2003), Empirical Ground-Motion Relations for Subduction-Zone Earthquakes and Their Application to Cascadia and Other Regions *Bulletin of the Seismological Society of America*, 93: 1703 – 1729

Boore, D.M. and Atkinson, G.M., 2008, Ground-Motion Prediction Equations for the Average Horizontal Component of PGA, PGV, and 5%-Damped PSA at Spectral Periods between 0.01 s and 10.0 s, *Earthquake Spectra*, 24(1), 99-138

Building Seismic Safety Council (BSSC) (2000), The 2000 NEHRP Recommended Provisions for New Buildings and Other Structures, Part I (Provisions) and Part II (Commentary), FEMA 368/369, Washington DC

Chiou, B. S.-J. and Youngs, R.R. 2008, An NGA model for the average horizontal component of peak ground motion and response spectra, *Earthquake Spectra,* 24(1) 173–215

McVerry, G.H., Zhao, J.X., Abrahamson, N.A., and Somerville, G.H., 2006, Crustal and Subduction zone attenuation relations for New Zealand earthquakes. *Bulletin of the New Zealand Society for Earthquake Engineering*, 39:(1), 1-58

Somerville, P.G., Smith, N.F. and Graves, R.W. 1994, The effect of critical Moho reflections on the attenuation of strong motion from the 1989 Loma Prieta, in "The Loma Prieta, California, Earthquake of October 17, 1989 - Strong Ground Motion," U.S.G.S. Professional Paper 1551-A, A67-A75

Youngs, R.R., Chiou, S.-J., Silva, W.J. and Humphrey J.R. 1997, Strong ground motion attenuation relationships for subduction zone earthquakes. Seismological Research Letters, 68(1): 58-73

Zhao, J.X., J. Zhang, A. Asano, Y. Ohno, T. Oouchi, T. Takahashi, H. Ogawa, K. Irikura, H.K. Thio, P.G. Somerville, Yasuhiro Fukushima, and Yoshimitsu Fukushima 2006a, Attenuation relations of strong ground motion in Japan using site classification based on predominant period. *Bulletin of the Seismological Society of America*, 96, 898-913.

Zhao, J.X., Irikura, K., Zhang, J., Fukushima, Y., Somerville, P.G., Asano, A., Ohno, Y., Oouchi, T., Takahashi, T. and Ogawa, H. 2006b, An empirical site classification method for strong motion stations in Japan using H/V response spectrum ratio. *Bulletin of the Seismological Society of America*, 96, 914-925.